# The effects of aperture distribution and compression on transport properties in rock fractures

*Joseph Ho Yin Ma*, Yunyue Elita Li and Arthur Cheng (National University of Singapore)*

**Summary**

The transport properties in rock fractures depend on the aperture size and its distribution. The ability to infer fracture aperture distribution from flow data would provide significant amount of information for reservoir characterization and monitoring. In this study, fluid flow and transport properties are carefully examined using numerical simulations on rough rock fractures, whose the aperture distributions are controlled by surface height variance, its autocorrelation length, and the external compression state. It was found that 1) combinations of different autocorrelation lengths and surface variances yielded fractures of distinct effective permeability; 2) unique definition of the rough fracture cannot be resolved using flow and transport properties at a static compressional state; and 3) transport properties under different compressions could be used to better constrain the aperture distribution.

**Introduction**

Changes in fracture dimension between rock surfaces have important impacts over the flow behaviour and elastic moduli of the effective medium. Fractures provide good passageway for fluids to move across between the rock surfaces and thus its dimension affects the permeability and hydraulic conductivity [Brown, 1987; Zimmerman et al., 1990]. At the same time, changes in fracture dimension due to external stresses not only reflect the change in contact area between the rock surfaces, but also leads to a difference in its capability to include fluids. Therefore, the elastic moduli of effective medium are closely related to fracture dimension as well [Swan, 1983].

In a simple conceptual illustration, a fracture is referred as the void space existing between two rock surfaces. The dimension of fracture is determined by the relative roughness of two rock surfaces, and could be described by the local aperture heights, which is the difference in displacement between the two constituting rock surfaces. Changes in external stress could alter the fracture dimension, by changing the global or local aperture heights. For instance, compression between the two rock surfaces tends to reduce the aperture height [Brown, 1986] and could even close some apertures when two surfaces are in contact. As a result, changes in fracture dimension are not just altering the width of flow paths, but could also provide extra or eliminate pre-existing flow paths. Kang et al. [2016] showed the emergence of preferential flow paths and anomalous transport behaviour across a stressed applied fracture.

In this study, we attempted to investigate 1) how the fluid transport properties in fracture medium were affected by compression of rock surfaces with different aperture distributions; and 2) whether the transport characteristic properties under different fracture compression could be used to infer the roughness of rock surfaces, and thus the heterogeneity of fracture apertures.

**Methods**

Dimensionless simulations were considered in this study. First, we considered a single isotropic joint fracture, formed between two rock surfaces in a square domain with length $L$, where the upper surface ($S_1$) is flat and lower surface ($S_2$) is rough. The lower surface $S_2$ was assumed to follow, and randomly generated from, a lognormal distribution where the roughness is determined by $S_2$ variance ($\sigma_0^2$) and its autocorrelation length ($\lambda$) [Ruan and McLaughlin, 1998]. The aperture height ($h$) of the fracture was given by the non-negative displacement of the two surface:

$$h(x,y) = \max\{0, S_1(x,y) - S_2(x,y)\} \quad . \qquad (1)$$

Local permeability *(k)* was related to aperture height by:

$$k = Ch^2 \qquad (2)$$

where $C$ is a flow path dependent dimensionless constant. Water with density ρ and viscosity μ was taken as the transported fluid in fractures. These assumptions implied that the fracture hydraulic conductivity $K$ (under gravity $g$):

$$K = \frac{\rho g}{\mu} k \qquad (3)$$

also followed a lognormal distribution, and that the fluid flow rates related the aperture heights with a cubic law.

We then computed the steady state flow flux *(q)* in the corresponding fracture medium according to Darcy's Law

$$\vec{q} = -\frac{k}{\mu} \nabla P \qquad (4)$$

by applying constant normalized pressure across the domain boundaries respectively. This background flux field served as a basis for numerically solving the transport of particles across the domain with Continuous Time Random Walks (CTRW) model [Kang, 2011]. On left boundary of the fracture, we injected particles and allowed them to be transported through. Time required for the particles to exit at the right boundary were recorded. The probability densities of transported particles against time were referred to breakthrough curves, which provided useful information in characterizing the transport properties of the medium.

Taking into account of different aperture distribution, we considered $\sigma_0^2$ between 0.1 (relatively homogenous

surface) to 5 (very heterogeneous surface), and $\lambda$ between $L/50$ (patterns more repetitive) to $L/10$ (less repetitive). More importantly, to investigate the effect of compression of fracture on transport properties, we repeat these cases by lowering $S_1$ with a compression displacement ($d$) of 0 to $3.5\sigma_0$ respectively. In particular, $d = 0\sigma_0$ was referred to the reference compression state, where $S_1$ and $S_2$ were assumed to be just in touch, i.e. $S_1(x,y)|_{d=0} = \max\{S_2(x,y)\}$. A schematic illustration of our fracture dimension configuration was illustrated in Figure 1.

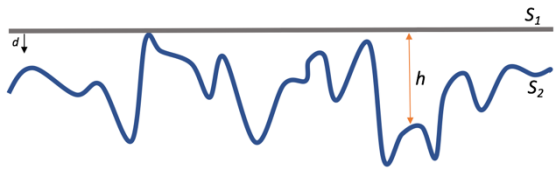


Figure 1: Schematic illustration of the reference fracture cross-section where apertures of height $h$ was formed from a flat upper surface ($S_1$) and a rough lower surface ($S_2$). $S_1$ was to be subjected to a compression displacement $d$.

**Effect on Fracture Permeability**

We examined the effective permeability of the fractures, which were calculated through the Darcy's Law based on total outgoing fluxed at the right boundary and pressure difference across the medium. Figure 2 showed the effective permeability of fracture with rock surface of different heterogeneity under reference compression states. The plots were given in log scale for the large magnitude variations among the fractures.

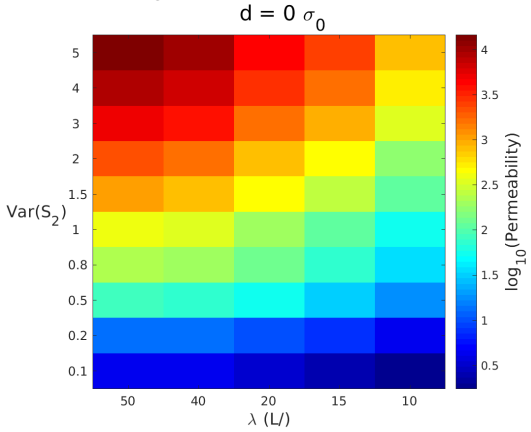


Figure 2: Effective permeability of fracture at vaiorus rock surface variance and correlations lengths at reference compression state.

It could be observed that at reference compression state, low permeability fractures were attained when they had low surface variance and high correlation lengths. This was resulted from low permeability flow paths due to distribution of apertures. Lower surface variance itself would result in a lower surface variation and consequentially, lower aperture heights. This had constrained the possibility of high permeability. In addition, longer correlation length implied that the micro-distributions of apertures were less repetitive inside the domain. In another word, the regions with low permeability would be more concentrated and larger in the domain. This created the necessity of longer paths to connect points with high permeability, thus having a greater potential in yielding more curved preferential flow paths. Hence, these conditions would lead to lower permeability fractures.

As the compression magnitude increases, the effective permeability decreases. This result was expected because as the increased compression narrowed the apertures, providing smaller cross-section area for fluid to transport across. In particular, it was observed that fractures that have high effective permeability at reference compression state are less affected by compression. Figure 3 showed the percentage changes in effective permeability of four fractures, which the effective permeability at reference compression state was high (14600, in yellow), low (1.75, in purple) and similar (1550, in blue and 1740, in red respectively) at their reference compression state. It showed that the fracture with high reference state effectively only experienced around 3.7% decrease in effective permeability under compression of $1\sigma_0$, and slightly more than 12.5% reduction under a $3.5\sigma_0$ compression. In a sharp contrast, the fracture with low reference state permeability from its high autocorrelation lengths and low surface variance suffered up almost to 42.5% effective permeability reduction at $1\sigma_0$ compression, and slightly more than 97.3% under a $3.5\sigma_0$ compression. For the two fractures with similar effective permeability, it was shown that the reduction were similar (23.6% and 27.2% respectively).

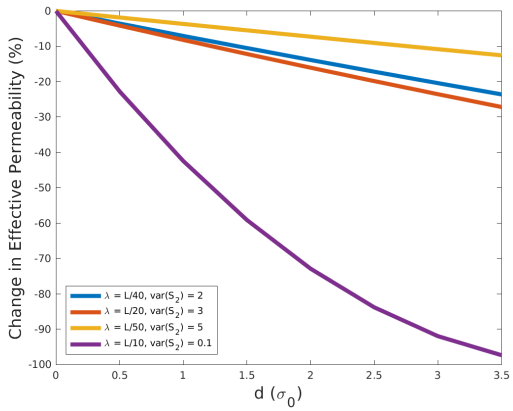


Figure 3: Percentage change in effective permeability under various compression magnitude for fractures with high (in yellow), low(in purple), and similar (in blue and red) effective permeability at reference compression state.

Since flow paths in fractures were likely to become curvier as apertures were more compressed and non-permeable zone emerged, the reductions in effectively permeability were especially significant on low permeability fractures which had higher tortuosity to begin with. In fact, Matyka et al. [2008] provided a relation which suggested that permeability would reduce with the square of tortuosity in a porous medium. This explained why certain fractures would have a much greater reduction in effective permeability under compression than others. Measuring changes in effective permeability provides extra information about the fracture surface distribution.

**Effect on Transport Properties**

To define a quantitative measure of the shape of the breakthrough curve, we used the quantity 90% confidence breakthrough interval, which was defined as the normalized time interval between 5% and 95% breakthrough. Cumulative breakthrough curves offered an easier way to extract this value. An example was provided as Figure 4. Higher value of confidence breakthrough interval implied a broader and heavier tailed breakthrough curve, representing stronger anomalous transport exhibited in the fracture.

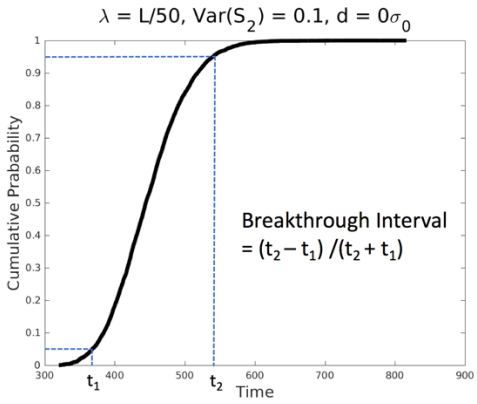


Figure 4: Example of cumulative breakthrough curve, and the corresponding breakthrough interval.

Figure 5 showed the breakthrough interval of fracture under reference compression states. It was observed in that in general a lower $S_2$ variance and a longer autocorrelation length led to a higher confidence breakthrough interval. The breakthrough interval for most combinations of surface variance and autocorrelation length resulted in a breakthrough interval between 0.14 and 0.18. Yet, on fractures with low surface variance and high correlation length, and thus low reference compression state effective permeability, the breakthrough intervals are higher and could be as high as 0.26. This implied the transport properties became much more anomalous under these conditions. In particular, the breakthrough intervals increased greater on scenarios that had higher breakthrough intervals at reference compression state.

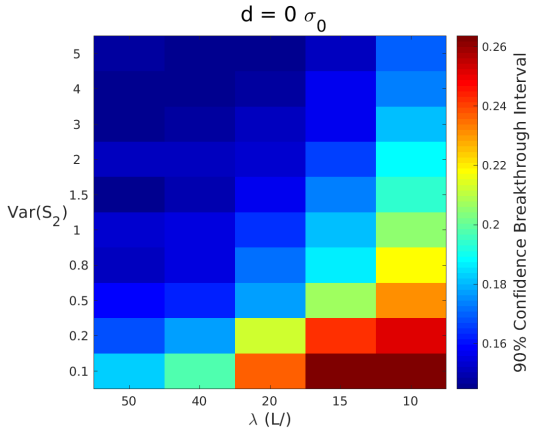


Figure 5: 90% Breakthrugh confidence interval of fracture at vaiorus rock surface variance and correlations lengths, under compression displacement of (a) $0\sigma_0$; and (b) $3\sigma_0$.

Comparing Figure 2 and Figure 5, the distribution of breakthrough intervals was observed to be correlated with the effective permeability of fractures. That is, high permeability usually corresponded to low breakthrough interval, and vice versa. This phenomenon could be understood as the readily available high permeability flow paths which had made the fractures high in effective permeability as discussed above. Background fluid flow fluxed at comparable among the available paths. The direction of particle transport was thus more aligned with the boundary pressure gradients, making most of them could pass the fracture at relatively similar amount of time. Therefore, the transport was more Fickian at these conditions. On the other hand, the fractures where surface variance are low and autocorrelation length are high would have more tortuosity due to more concentrated low permeability areas. This situation would concentrate preferential flow paths and resulted in more areas with background fluid acceleration or deceleration. Also, the breakthrough paths would be more dependent on initial injection point and so did the breakthrough time. These factors combined resulted in the occurrence of more anomalous transports in these fractures, which was reflected as longer breakthrough intervals.

Figure 5 was also suggested that similar breakthrough intervals could be attained in fracture with rock surface differ in these parameters, which might (circumstance I) or might not (circumstance II) have the similar effective permeability. For instance, at reference compression state, both the fractures of (A) $\sigma_0^2 = 2$, $\lambda = L/40$ and (B) $\sigma_0^2 = 3$, $\lambda = L/20$ had a breakthrough interval of 0.1508 at reference compression state. At the same time, these two fractures

have similar effectively permeability (155 against 174). For another situation, fracture (C) $\sigma_0^2 = 0.1$, $\lambda = L/50$ and (B) $\sigma_0^2 = 3$, $\lambda = L/10$ differed greatly in effective permeability (4.36 against 346), but they still had very close breakthrough interval at reference compression state had a breakthrough interval of 0.1508 at reference compression state (0.1824 against 0.1814). The similarly in breakthrough intervals had made it difficult to identify their rock surfaces and thus fracture heterogeneity if only the flow characteristics of one compression state was provided.

However, by including the information of extra fracture compression states, two fractures which originally shared similar sign in anomalous transports would become distinguishable. Figure 6 showed the changes in breakthrough interval of the four fractures these two circumstances under different compression displacement. The plot offered two aspects helpful for classification - overall breakthrough interval changes, and response under particular compression magnitude.

The solid lines in Figure 6 represented the fractures A and B under circumstance I. These fractures had similar effective permeability, and the changes of that were comparable, as revealed from Figure 3. Although under fracture compression of displacement less than $2\sigma_0$, the difference was still unclear, it was able to differentiate the two beyond compression displacement higher than $2.5\sigma_0$. The flow in fracture A eventually became slightly more anomalous than fracture B under high compression. In addition to the eventual changes of breakthrough interval, the changing response of breakthrough interval under different compression displacement might also serve as one of the clue for identification. Despite as revealed from Figure 3, both fractures have a rather constant trend of effective permeability reduction, the breakthrough interval changes did not entire correlate with that. For instance, the breakthrough interval of fracture A had a drop when $d$ increased from 2.5 to $3\sigma_0$, while in fracture B there was an abrupt spike in breakthrough interval when $d = 1\sigma_0$. These features were controlled by micro-variations in the aperture distribution under compression of different magnitudes, which could not be revealed only from changes in effective permeability as the quantity represented a domain average.

The differentiation of fracture heterogeneity would be more straightforward for fractures that have different effective permeability at reference compression state. This was because the aperture distribution variation resulted in the effective permeability difference would also lead to a distinctive response in anomalous transports upon compression. The dash-dotted line plots in Figure 6 represented fractures C and D in circumstance II, where they had major difference in effective permeability. It was obvious that the breakthrough interval of fracture C rose significant more rapid than fracture D. This implied that the flow in fracture C would have become way more anomalous under compression, as compared to fracture D. Therefore, the availability of transport behaviour measurements at various compression states would be useful to serve as another indicator in identifying both the heterogeneity of fracture and state of compression.

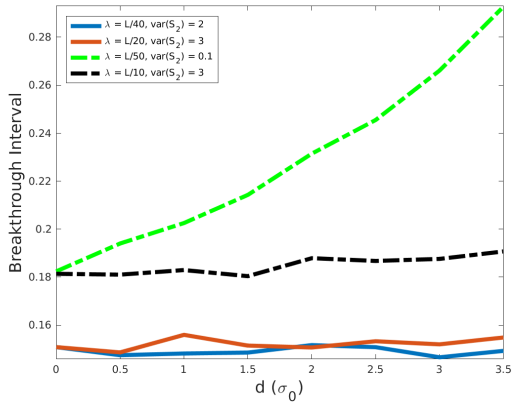


Figure 6: Changes in breakthrough interval of fractures which had similar breakthrough interval and similar effective permeability (in solid lines)/ but different effective permeability (in dash-dotted lines) under referecne comression state.

## Conclusions

It was discovered from this study by numerical simulations that low autocorrelation length and high surface variance would result in high permeability fractures. Similar flow and transport data may be observed with many different combinations of surface variance and autocorrelation length at a single compression state. Greater compression reduced the permeability of fractures to a different extent depending on the surface characterization. CTRW modeling suggested that low permeability fracture were more likely for anomalous transport to take place, where the transport became increasing anomalous under further compression. Lastly, as transport properties of fractures responded differently under various compression states, it was suggested that compression dependent flow and transport measurements were helpful in classifying the types of fracture heterogeneity.

## Acknowledgements

The authors acknowledge the EDB Petroleum Engineering Professorship for their financial support. Dr. Yunyue Elita Li is funded by MOE Tier-1 Grant R-302-000-165-133. Joseph Ma is supported with Singapore International Graduate Award by A*STAR. The authors also thank Dr. Peter Kang of KIST for his input with CTRW modelling.

**References**

Brown, S.R., 1987. Fluid flow through rock joints: the effect of surface roughness. *Journal of Geophysical Research: Solid Earth*, *92*(B2), pp.1337-1347.

Brown, S.R., Kranz, R.L. and Bonner, B.P., 1986. Correlation between the surfaces of natural rock joints. *Geophysical Research Letters*, *13*(13), pp.1430-1433.

Kang, P.K., Brown, S. and Juanes, R., 2016. Emergence of anomalous transport in stressed rough fractures. *Earth and Planetary Science Letters*, *454*, pp.46-54.

Kang, P.K., Dentz, M., Le Borgne, T. and Juanes, R., 2011. Spatial Markov model of anomalous transport through random lattice networks. *Physical review letters*, *107*(18), p.180602.

Matyka, M., Khalili, A. and Koza, Z., 2008. Tortuosity-porosity relation in porous media flow. *Physical Review E*, *78*(2), p.026306.

Ruan, F. and McLaughlin, D., 1998. An efficient multivariate random field generator using the fast Fourier transform. *Advances in water resources*, *21*(5), pp.385-399.

Swan, G., 1983. Determination of stiffness and other joint properties from roughness measurements. *Rock Mechanics and Rock Engineering*, *16*(1), pp.19-38.

Zimmerman, R.W., Chen, D.W., Long, J.C.S. and Cook, N.G.W., 1990, June. Hydromechanical coupling between stress, stiffness and hydraulic conductivity of rock joints and fractures. In *Rock Joints Proc. Inter. Symp., Balkema, Leon, Norway*.